

Risk Assessment of Bird Collisions with a Wind Turbine Based on Flight Parameters

Grzegorz Madejski¹, Rafal Tkaczyk¹, Dawid Gradolewski¹, Damian Dziak¹, Wlodek J. Kulesza^{2,*}

¹Bioseco S. A.,

Budowlanych 68, 80-298 Gdansk, Poland

²Department of Mathematics and Natural Sciences, Blekinge Institute of Technology,
371 79 Karlskrona, Sweden

grzegorz.madejski@bioseco.com; rafal.tkaczyk@bioseco.com; dawid.gradolewski@bioseco.com;
damian.dziak@bioseco.com; *wlodek.kulesza@bth.se

Abstract—The study addresses the challenge of bird collisions with wind turbines by developing an autonomous risk assessment method. The research uses data from the stereoscopic Bird Protection System (BPS) to anticipate potential collision threats by analysing flight parameters and distance from turbines. The danger factor depends on the flight characteristics of the identified bird species and the parameters of the wind turbine control system. The paper proposes an online quantitative risk assessment model that operates in real time, with the aim of minimising unnecessary turbine shutdowns while improving bird conservation. The model is validated through field data from bird flights. The findings suggest that adaptive management of turbine operations based on real-time bird flight data can significantly reduce collision risks without compromising energy production efficiency. The research underscores the balance between ecological considerations and the economic viability of wind energy, proposing an adaptive strategy that reduces unnecessary turbine stoppages while ensuring the safety of avian species.

Index Terms—Collision risk; Damage collision avoidance; Green energy; Energy efficiency; Nature conservation sustainability; Wind farm.

I. INTRODUCTION

The detection, localisation, and identification of flying objects are subjects of interest to scientists and modern industry, who are aware of societal demands, trends, and growing market needs. Potential application areas include environmental risk management at airports, preinvestment environmental studies, infrastructure security, and bird protection at wind farms. The last area is also a milestone in the European Green Deal and biodiversity protection during the ongoing energy transition [1].

The efficiency of bird protection at wind farms is no longer an issue, and state-of-the-art solutions such as Bioseco Bird Protection Systems (BPS) [2] or IdentiFlight [3] have already been tested against challenging requirements determined by a recognised environmental consultancy agency such as the

Manuscript received 11 March, 2024; accepted 27 June, 2024.

This research was funded by The National Centre for Research and Development of Poland under Grant No. POIR.01.02.00-00-0247/17. Project title: “Realization of R&D works leading to the implementation of a new solution—MULTIREJESTRATOR PLUS for monitoring and control of the power system in terms of operational efficiency, the life span extending and optimizing the impact on the surrounding wind farms”.

Kompetenzzentrum Naturschutz und Energiewende (KNE) in Germany [4] or the MAPE project in France [5].

Local environmental authorities determine the required detection range of the system, which depends on the flight direction and speed of protected species at a given location and the time necessary to stop or slow down an erected wind turbine (WT). The detection range can be set with the use of the following equation

$$R_T = f_{RDE} \times V_{o_{max}} \times (T_{reaction} + T_{latency}), \quad (1)$$

where $V_{o_{max}}$ is the measured speed of birds toward a turbine, $T_{reaction}$ is the reaction time needed to stop or slow down the turbine, $T_{latency}$ is the latency time of a bird detection system, and f_{RDE} is the coefficient of relative distance error (RDE) associated with the positioning error of the data acquisition system. In extreme cases, like a red kite, which moves at an average speed of 10 m/s, and a large WT that stops can even take 45 seconds, the detection range exceeds 450 meters.

Nowadays, in bird-sensitive locations, aviation detection systems can frequently stop the turbine, even when birds are not on a collision trajectory with the turbine or are flying slower than the assumed maximum speed. Rigid requirements do not consider situations where the turbine is spinning relatively slowly and can be stopped fast or when the bird is flying against the wind direction, which postpones the possible collision instant.

The research gap has recently been recognised by the German government and the KNE organisation, and the economic viability of the implemented solution has become a primary consideration in the decision-making process, since “economic considerations are increasingly important in selecting measures” [4]. For BPS to be widely applied in the future, it must demonstrate effectiveness in collision avoidance and comply with specific price limits. These price limits account for the system costs and energy production losses due to detection.

Based on the motivation presented, the research aims to develop an autonomous risk assessment method that can identify potential threat levels at an early stage using the distance from a turbine and speed estimates derived from stereoscopic BPS data.

II. BACKGROUND KNOWLEDGE AND RELATED WORKS

There are many types of sensors that can provide reliable information about the position of flying objects for risk assessment in critical infrastructure, such as wind farms or airports. The most widely used are GPS, radars, lidar, cameras, and vision systems [3], [6]–[10].

In [6], [7], a GPS-based method of tagging birds to log their flight trajectories is described. The main advantage is constant and reliable monitoring of the location of the object with a relatively small uncertainty of ± 10 m. However, due to its technical limitations, it is mostly used for scientific purposes.

The authors in [8] develop the radar-based solution to predict the risk of bird strike. This approach provides good measurement over long distances and is resistant to view conditions such as weather and time of day.

Another approach is based on vision sensors when a monocular system activates the deterrence once the object is detected [11], [12]. Most advanced stereovision-based solutions allow mitigating the collision risk based on the position of a bird and its estimated size [2], [13]. Recent technologies allow differentiation of action needs based on the automatically identified bird species [9], [10].

The stereovision-based solution has been used to analyse the behavioural and morphological features of birds to determine the risk of species-specific collisions at wind farms [9], [14]. Four features have been extracted for the risk assessment: head position, active flight, track symmetry, and track tortuosity. The Akaike information criterion was used as a prediction error estimator. Research has shown that trajectory analysis depends on flight height and tortuosity. Both factors are interconnected, and for instance, migratory birds with straight trajectories fly statistically higher than others.

The authors in [6] investigate the impact of altitude measurement on the assessment of collision risk. They use the kernel utilisation distribution method and the probability density of birds in a given area to determine the risk that a specific species occurs in a given area and estimate their activity throughout the year. This approach is useful when scheduling WT run-time or planning the deployment of new WT. In [15], it is emphasised that changes introduced in an existing farm, or the creation of a new one affect the behaviour of birds in other wind farms. This means that the statistical risk models for wind farms must be updated periodically.

Another approach to mitigate the impacts of wind farms on birds is described in [10]. This solution uses modelling techniques, including maximum entropy models (MAXENT) and generalised linear models (GLM), to create a species distribution model. Based on this, risk maps were generated to identify areas where the presence of the species is likely and where there is a high risk of mortality.

The solution proposed by Metz *et al.* [8] uses radar data with a linear regression model to predict the trajectories of birds in real time. The closest point of approach (CPA) between the bird and the aircraft is calculated. The collision probability is then estimated based on the predicted bird trajectory, location uncertainty, and arrival time at the CPA. The final stage provides the expected severity of the collision calculation, i.e., if probability and severity exceed predefined

thresholds, then the aeroplane is delayed until the risk is mitigated.

III. PROBLEM STATEMENT, OBJECTIVES, AND MAIN CONTRIBUTIONS

The review of related works shows several approaches to assessing the risk of birds' collision with man-made infrastructure. Most of them operate offline or do not provide a clear quantitative risk measure. The main goal of this research is to propose an online quantitative risk assessment method that considers all the constraints related to wind turbine bird collision prevention. The main objective of the solution is to improve bird preservation without compromising the economic aspects of energy losses due to unnecessary turbine stopping. Our approach deals with the three research questions defined below.

The first question concerns which measurable flight parameters are most useful for a reliable risk assessment of bird collisions with a man-made infrastructure and which constraints related to the monitored infrastructure are crucial for the real-time risk collision assessment.

We assume that the current radial distance and temporal radial velocity are the most suitable and robust flight parameters for the risk collision assessment in real time. The parameters are defined in a spherical coordinate system with the centre of a wind turbine tower. The necessary action time to prevent the collision can be a constraint related to the monitored infrastructure, which is crucial for real-time risk collision assessment.

The second question is related to the danger map model, which is useful for handling the control with suitable reliability.

We propose to apply a statistical model that relates the risk to the actual radial distance R along with the instant radial flight speed V_R to the known maximum flight velocity of the identified bird species V_{max} and the maximum time needed to stop the turbine T_{action} .

The third research question asks about the structure of the system, which estimates the robust parameters for risk analysis and estimates a danger factor.

This system can be based on the stereovision system with embedded data preprocessing for signal enhancement, ensuring a precise estimation of the position and velocity of the flying object.

The main contribution of the paper is to propose a model for assessing collision risk, including uncertainty analysis. Furthermore, the model is implemented on a real-time stereovision system for bird monitoring. The model is validated using real data from bird flights and fixed-wing drones equipped with GPS.

IV. MODELLING OF COLLISION RISK ASSESSMENT

The risk of bird collision with the wind turbine can be expressed as a product of two dynamic factors: *Position* associated with the localisation of the object in the danger zone, the *Velocity* that characterises the movement of the object, and the parameters that define the turbine control system.

The risk probability \mathbb{P}_{risk} (2) depends on the object's category, including characteristics of particular bird species such as size and maximum flight speed. It also depends on the

position of the object in terms of its distance from the plane of the collision target and the actual velocity toward the turbine

$$\mathbb{P}_{risk} = f(R, R_T, V_R, V_{max}, T_{action}), \quad (2)$$

where R is an instant radial distance between the object and the turbine, R_T is a risk collision radial distance for the maximum speed of the object, V_R is the radial speed of the object, V_{max} is the maximum possible speed of the object, $T_{action} = T_{reaction} + T_{latency}$.

The turbine must be slowed down when the object reaches the distance R_T to the turbine, which the bird can reach at a given flight speed. The maximum risk distance for a given bird species can be calculated using the following equation

$$R_T = V_{o_{max}} \times T_{action}, \quad (3)$$

where $V_{o_{max}}$ is the maximum flight speed of the detected and identified bird species or another detected object on the collision path.

We assess the risk of collision using the danger factor, DF , which depends on the speed of the object towards the turbine and the distance from the collision. It can be estimated using the following equation

$$DF = \frac{R_T}{R} \times \frac{V_R}{V_{R_{max}}} = \frac{V_{R_{max}} \times T_{action}}{R} \times \frac{V_R}{V_{R_{max}}} = \frac{V_R}{R} \times T_{action}, \quad (4)$$

where R is an instant radial distance between the object and the turbine, R_T is a risk collision radial distance for the maximum speed of the object, V_R is the radial speed of an object towards the turbine, and $V_{R_{max}}$ is a risk collision distance for the maximum speed of the object.

The function values are truncated in the interval $[-1, 1]$, where the values from 0 to 1 indicate an increasing level of risk and the values from 0 to -1 denote increasing levels of safety, i.e., when a bird is flying in the opposite direction to the collision sphere. Therefore, the *DangerLevel* can be defined as

$$DangerLevel = \begin{cases} DF & \text{if } R > |V_R| \times T_{action}, \\ \text{sign}(V_R) & \text{if } R \leq |V_R| \times T_{action}. \end{cases} \quad (5)$$

To estimate the uncertainty of the *DangerLevel*, we calculate a geometric sum of partial differences to the modified (4)

$$DF = \frac{R_2 - R_1}{R_1 \Delta T} \times T_{action}. \quad (6)$$

Therefore,

$$\begin{aligned} \Delta DF &= \sqrt{\left(\frac{\delta DF}{\delta R_1} \Delta R_1\right)^2 + \left(\frac{\delta DF}{\delta R_2} \Delta R_2\right)^2} \approx \\ &\approx \sqrt{2} \times \frac{T_{action}}{\Delta T} \times \frac{\Delta R}{R} = \sqrt{2} \times \frac{T_{action}}{\Delta T} \times \frac{R}{fb} \times \Delta p_x, \end{aligned} \quad (7)$$

since

$$\Delta R = \frac{R^2}{f \times b} \times \Delta p_x, \quad (8)$$

where R_1 and R_2 are radial distances at the beginning and end of the trajectory part at which an average radial velocity V_R is calculated, ΔT is the period for which the velocity is estimated, ΔR , ΔR_1 , ΔR_2 are quantisation errors at distance R , R_1 , R_2 , respectively, $R = (R_1 + R_2)/2$, b is a baseline, f is a focal length, and Δp_x is a pixel size.

To reduce the uncertainty caused by the quantisation error, one can estimate ΔDF based on N samples with longer averaging ΔT , then

$$\Delta DF \approx \sqrt{2} \times \frac{T_{action}}{\Delta T} \times \frac{R}{fb} \times \frac{\Delta p_x}{N}. \quad (9)$$

As illustrated in Fig. 1, the radial speed can also be presented as a vector \vec{V}_R consisting of three components: one vertical and two horizontal, one towards the plane of turbine blades and one parallel to the turbine blades plane

$$\vec{V}_R = \vec{V}_{R_v} + \vec{V}_{R_{H_1}} + \vec{V}_{R_{H_2}}, \quad (10)$$

where \vec{V}_R is the radial speed of the detected bird in the stereo camera direction, \vec{V}_{R_v} is a vertical component of the radial speed, $\vec{V}_{R_{H_1}}$ is a horizontal component of the radial speed towards the blades' plane, and $\vec{V}_{R_{H_2}}$ is a horizontal component of the radial speed parallel to the blades' plane.

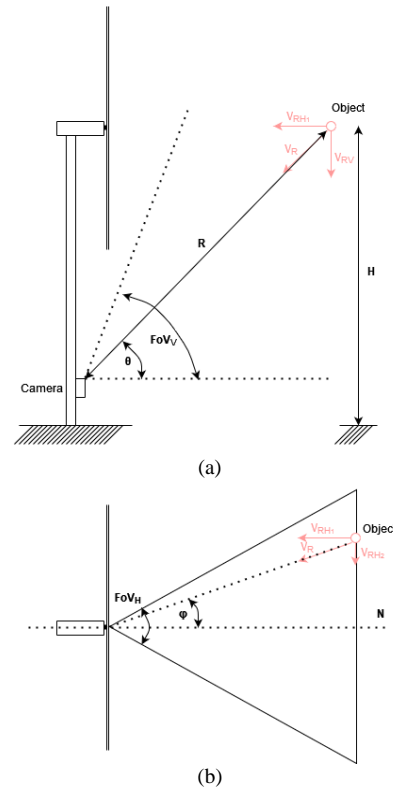


Fig. 1. An illustration of the camera views of the object from the side (a) and top (b) views, where FoV_v is a vertical field of view, ϕ is the azimuth angle, θ is the polar angle, and H is the height of the position of the object.

The worst-case situation is when the bird is flying towards the blades, which are particular to the camera's optical axes. The horizontal speed component towards the wing plane is the component creating the risk. This component can be calculated from the following equation

$$\vec{V}_{R_{H_1}} = \vec{V}_R \times \cos \varphi \times \sin \theta, \quad (11)$$

where θ is a polar angle and φ is an azimuthal angle.

The same relationship can be applied to the radial distance and its vectorial components. Therefore, since the *DangerLevel* is a relative value and its numerator and denominator depend on radial distance, azimuthal and polar angles do not impact the presented risk analysis.

Considering the impact of uncertainty ΔDF on risk estimation, the distance when the action has to be taken for a given bird species can be estimated from the equation

$$\frac{V_R}{R} \times T_{action} - \sqrt{2} \times \frac{T_{action}}{\Delta T} \times \frac{R}{fb} \times \frac{\Delta p_x}{N} = 1. \quad (12)$$

Figure 2 shows the implementation of a safety map model, where the danger factor is related to the distance R and the velocity V_R for the given species and the characteristics of the turbine. In the figure, the uncertainty of the estimation is represented as an increase with an R margin around the critical value 1. For the analysis, we assume that the turbine needs 20 seconds to stop and that the averaging time of velocity estimation is two seconds.

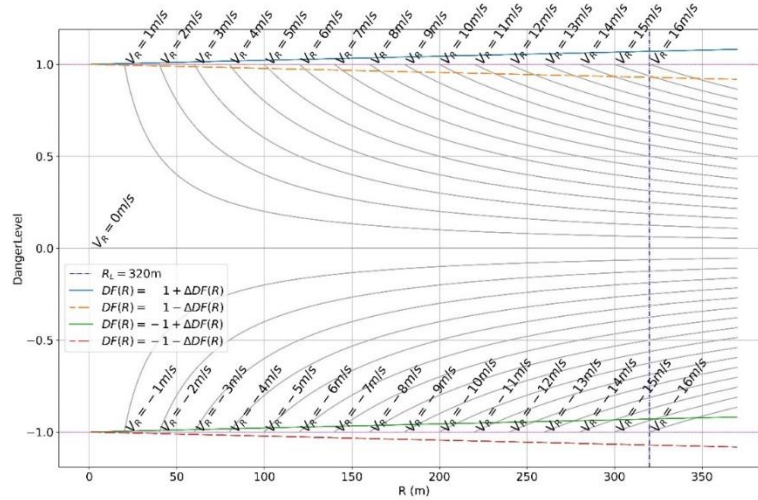


Fig. 2. A risk map for $\Delta T = 2$ s, $N = 32$, $T_{action} = 20$ s, $V_{max} = 16$ m/s. The estimation uncertainty is presented as arms of the angles around the lines $DF = 1$ and $DF = -1$.

From Fig. 2, one can see that to stop the turbine for the maximum red kite flight velocity $V_R = 16$ m/s, the critical distance R_L is 320 m. However, because of the uncertainty of the estimate, it has to be done at a distance of about 350 m. The difference of 10% for all velocities is a reasonable approximation of the estimate.

V. VALIDATION

The proposed method was tested on real data provided by a Bioseco BPS *long-range* version installed at a wind farm in northern Germany shown in Fig. 3. This is a bird-sensitive

area with high activity of red kites and white-tailed eagles nested nearby, which causes many turbines to stop with the conservative approach determined by (1). The system comprises eight detection modules installed around the tower to cover 360° viewing. Each module includes two pairs of stereovision cameras providing 66° vertical FoV_v. The baseline, $b = 1$ m, and the focal length, $f = 8$ mm. The vision sensor size (VSS) is 6.287 mm \times 4.712 mm, and the vision sensor resolution (VSR) is 4056 px \times 3040 px. The system detects and tracks multiple objects and estimates their size and spatial position [2].



Fig. 3. The Bioseco BPS *long-range* system at the test site used for system validation.

A fixed-wing drone equipped with GPS was used to verify the usability of a proposed risk estimation method. The flight path of the drone was designed to verify the accuracy of the BPS at distances from 100 m to 400 m and altitudes from 20 m to 120 m. From the provided data, the drone's radial speed in a direction towards the turbine \vec{V}_R and its position R were estimated in a spherical coordinate system.

Figure 4 shows the data processing flow chart. Two data sources were used: raw BPS data and a GPS log file. The BPS data include the pixel values of the centre of the detected object (x, y) and the timestamp t of each stereovision camera. The GPS log file contains the position parameters of the drone, i.e., latitude, longitude, altitude, and timestamp.

The raw data are preprocessed using *oversampling* and *filtering* algorithms to reduce noise and improve the signal-to-noise ratio. Since the BPS system operated at 16 FPS, the oversampling rate was set to 16 Hz, allowing the removal of small signal discontinuities due to possible missing detection samples. The effect of using a low-pass filter applied to the disparity of the disparity signal from the stereo camera is presented in Fig. 5.

One of the causes of uncertainty in distance measurement using stereovision is lean distortions. To eliminate this problem, only the central part of the image has been used in the analysis. Although such an approach reduces the FoV of the system, there are methods to mitigate the problem; however, this is beyond the scope of this paper.

Since using the spherical coordinate system is less sensitive to distance quantisation error, the analysis is based on this approach. In Fig. 1, the spherical reference centre is placed at a vision system installed at the bottom of the turbine.

After preprocessing, the position of the object is represented by the radial distance R , the polar θ , and the azimuthal angle φ . The derivative of the radial distance R is a measure of the radial velocity V_R of an object approaching or moving away from the turbine.

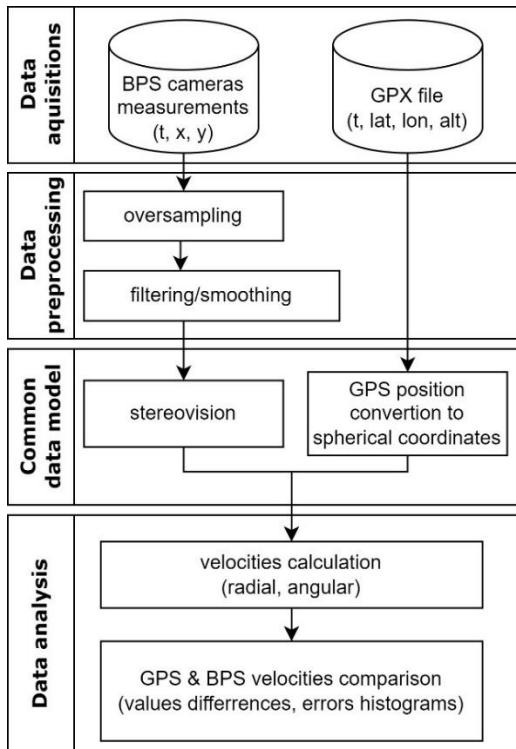


Fig. 4. Flow chart of the data analysis process.

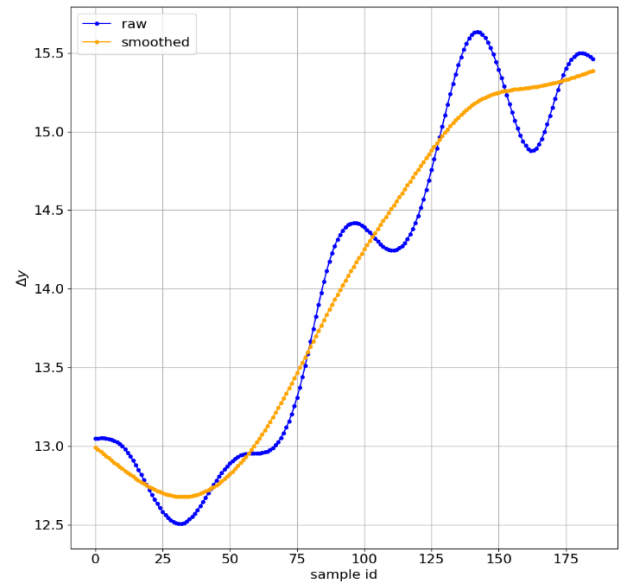


Fig. 5. Effect of using a low-pass filter on the disparity signal of the stereo camera.

To understand and evaluate the risk analysis, we need to verify the reliability of the measurement of its two main components: the radial distance R and its derivative, the radial velocity V_R . The uncertainty of distance measurement has already been validated and verified in recent studies with fixed-wing drone and ornithological observations [2], [13]. Figure 6 shows the flow of the radial velocity calculated from the GPS data of the drone's test flight (red line), which is compared with the results from raw Bioseco BPS data (blue line), later smoothed by an averaging method (yellow line). The Time limits define the FoV limitation caused by the lens distortion. In the defined time frame, the developed model meets the requirements determined in (5).

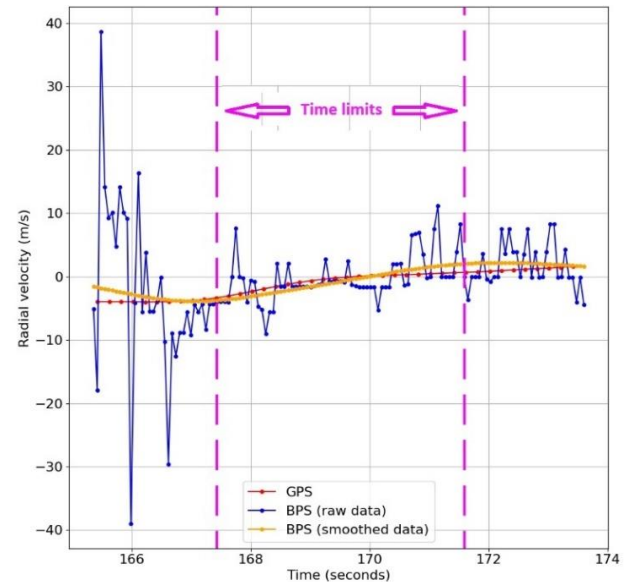


Fig. 6. Comparison of radial velocity V_R data from drone test flight using GPS and BPS data.

Figures 7 and 8 present the movements of red kites and kestrels, respectively. The maximum horizontal velocity of a red kite was set at $V_{max} = 16$ m/s. The processing time of SCADA and BPS $T_{Action} = 20$ s, and a 2 s averaging window of 32 samples are set. This results in a risk zone of $R_L = 320$ m. In the case of kestrels, whose $V_{max} = 11$ m/s, the

risk zone reaches $R_L = 230$ m.

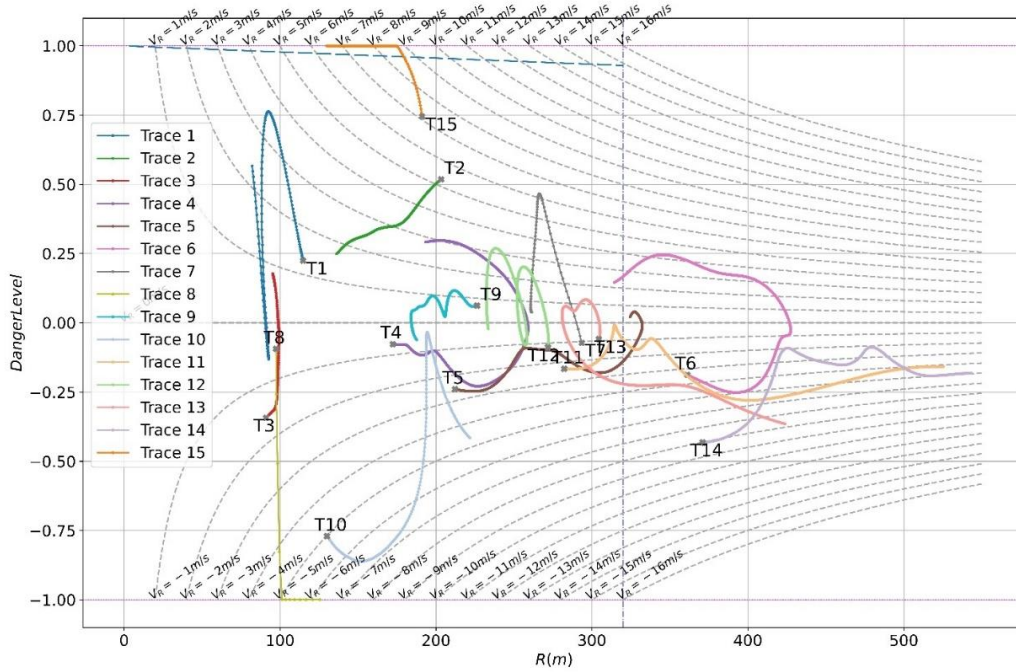


Fig. 7. A red kite danger map for $\Delta T = 2$ s, $N = 32$, $T_{\text{action}} = 20$ s, $V_{\text{max}} = 16$ m/s, $R_L = 320$ m. The dots mark the beginning of the trace.

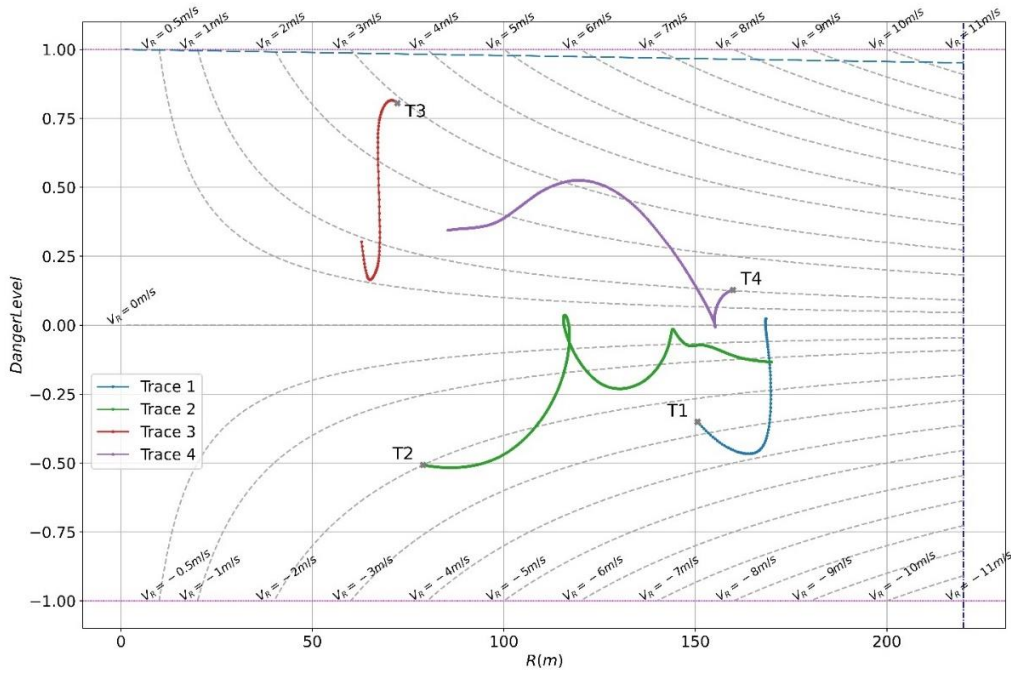


Fig. 8. A kestrel danger map for $\Delta T = 2$ s, $N = 32$, $T_{\text{action}} = 20$ s, $V_{\text{max}} = 11$ m/s, $R_L = 220$ m. The dots mark the beginning of the trace.

From Fig. 7 and Fig. 8, one can see that the birds have flown at a speed much lower than the maximum speed. In the case of red kites, the maximum measured speed was about 9 m/s. For kestrels, the maximum observed speed was about 3 m/s.

VI. DISCUSSION

As Fig. 7 shows, all red kite traces, except for trace 14, lie within the circle of R_L . When using a conservative approach with stopping a turbine whenever a bird flies within the R_L circle, the turbine would be stopped in 93.3% of the presented cases. However, using the proposed adaptive model with *DangerLevel* estimation, only the red kite in trace 15 would

trigger the turbine stop signal when $DangerLevel > 1 - \Delta DF$. This means that using the novel approach would reduce the stopping turbine in 92.9% of cases. This proves how much the implementation of the presented model can improve the efficiency of wind farms compared to the conservative approach of stopping the wind turbines for the worst-case scenario assuming the maximum flight speed towards a turbine.

The proposed approach to the management of collision risk can also be easily implemented, one needs to measure the radial distance and velocity and adjust the stopping instant to the flight speed of the bird. It provides transparent information not only about the danger factor, but, above all,

is useful in analysing the behaviour of birds in the vicinity of wind turbines.

VII. CONCLUSIONS

This paper presents a transparent risk assessment method for bird collisions with wind turbines. The research shows the efficiency of using spherical coordinates in mitigating distance quantisation errors, providing reliable radial distance and radial velocity measurements. To achieve this goal, proper preprocessing of BPS data is important, i.e., smoothing stereovision camera raw data by a low-pass filter and discarding samples aberrated by lenticular distortions.

The comparison of GPS and BPS data provides accurate radial distance and radial velocity samples, which is crucial for reliable risk assessments. This reliability is evidenced by the consistency observed between the two data sources.

The statistical analyses of the radial velocity and radius measurements validate the accuracy of the models, taking into account measurement errors and uncertainties. This validation reinforces the credibility of the proposed risk assessment methodology. This study is a solid preliminary for ongoing research in the mitigation of bird collision risk at wind farms. The expected final result should provide mutual benefits for bird conservation and optimal energy production by mitigating WT stops, and therefore the number of collisions.

Future work should focus on refining the risk assessment models by integrating additional factors, e.g., weather conditions, bird behaviour features, bird flight patterns, species classification, and external system information to increase prediction accuracy. Expanding the risk estimation equation to include more complex behavioural and environmental factors will provide a more comprehensive understanding of collision risks.

CONFLICTS OF INTEREST

The authors declare that they have no conflicts of interest.

REFERENCES

- [1] E. Fraccaro, "Green Deal and the European Biodiversity Strategy". [Online]. Available: https://environment.ec.europa.eu/strategy/biodiversity-strategy-2030_en

- [2] D. Gradolewski *et al.*, "Comprehensive bird preservation at wind farms", *Sensors*, vol. 21, no. 1, p. 267, 2021. DOI: 10.3390/s21010267.
- [3] B. W. Rolek, M. A. Braham, T. A. Miller, A. E. Duerr, T. E. Katzner, and C. J. W. McClure, "Variation in flight characteristics associated with entry by eagles into rotor-swept zones of wind turbines", *Ibis*, vol. 166, no. 1, pp. 308–314, 2024. DOI: 10.1111/ibi.13264.
- [4] E. Bruns, E. Schuster, and J. Streiffeler, "Anforderungen an technische überwachungs- und abschaltssysteme an windenergieanlagen: Abschlussbericht der workshopreihe "technische systeme", Kompetenzzentrum Naturschutz und Energiewende, 2021. DOI: 10.19217/skr610.
- [5] C. Ballester, S. M. Dupont, A. Corbeau, T. Chambert, O. Duriez, and A. Besnard, "A standardized protocol for assessing the performance of automatic detection systems used in onshore wind power plants to reduce avian mortality", *Journal of Environmental Management*, vol. 354, art. 120437, 2024. DOI: 10.1016/j.jenvman.2024.120437.
- [6] S. Khosravifard, A. K. Skidmore, B. Naimi, V. Venus, A. R. Muñoz, and A. G. Toxopeus, "Identifying birds' collision risk with wind turbines using a multidimensional utilization distribution method", *Wildlife Society Bulletin*, vol. 44, no. 1, pp. 191–199, 2020. DOI: 10.1002/wsb.1056.
- [7] T. Schaub, R. H. G. Klaassen, W. Bouten, A. E. Schlaich, and B. J. Koks, "Collision risk of Montagu's Harriers (*Circus pygargus*) with wind turbines derived from high-resolution GPS tracking", *Ibis*, vol. 162, no. 2, pp. 520–534, 2020. DOI: 10.1111/ibi.12788.
- [8] I. C. Metz, J. Ellerbroek, T. Mühlhausen, D. Kügler, and J. M. Hoekstra, "Analysis of risk-based operational bird strike prevention", *Aerospace*, vol. 8, no. 2, p. 32, 2021. DOI: 10.3390/aerospace8020032.
- [9] A. C. Linder, H. Lyhne, B. Laubek, D. Bruhn, and C. Pertoldi, "Modeling species-specific collision risk of birds with wind turbines: A behavioral approach", *Symmetry*, vol. 14, no. 12, p. 2493, 2022. DOI: 10.3390/sym14122493.
- [10] S. Smeraldo *et al.*, "Modelling risks posed by wind turbines and power lines to soaring birds: The black stork (*Ciconia nigra*) in Italy as a case study", *Biodiversity and Conservation*, vol. 29, no. 6, pp. 1959–1976, 2020. DOI: 10.1007/s10531-020-01961-3.
- [11] "DTBird website". [Online]. Available: <https://www.dtbird.com/>
- [12] "Biodiv-Wind home - Biodiv-Wind". [Online]. Available: <https://www.biodiv-wind.com/>
- [13] D. Gradolewski, D. Dziak, D. Kaniecki, A. Jaworski, M. Skakuj, and W. J. Kulesza, "A runway safety system based on vertically oriented stereovision", *Sensors*, vol. 21, no. 4, p. 1464, 2021. DOI: 10.3390/s21041464.
- [14] A. C. Linder, H. Lyhne, B. Laubek, D. Bruhn, and C. Pertoldi, "Quantifying raptors' flight behavior to assess collision risk and avoidance behavior to wind turbines", *Symmetry*, vol. 14, no. 11, p. 2245, 2022. DOI: 10.3390/sym14112245.
- [15] K. Reid, G. B. Baker, and E. J. Woehler, "An ecological risk assessment for the impacts of offshore wind farms on birds in Australia", *Austral Ecology*, vol. 48, no. 2, pp. 418–439, 2023. DOI: 10.1111/aec.13278.



This article is an open access article distributed under the terms and conditions of the Creative Commons Attribution 4.0 (CC BY 4.0) license (<http://creativecommons.org/licenses/by/4.0/>).